Delft University of Technology

Exciting Nonlinear Modes of Conservative Mechanical Systems by Operating a Master Variable Decoupling

Santina, Cosimo Della; Lakatos, Dominic; Bicchi, Antonio; Albu-Schaeffer, Alin

Important note
To cite this publication, please use the final published version (if applicable).
Please check the document version above.

Exciting Nonlinear Modes of Conservative Mechanical Systems by Operating a Master Variable Decoupling

Cosimo Della Santina[1,2], Dominic Lakatos[1], Antonio Bicchi[3], Alin Albu-Schaeffer[1,4]

Abstract— Eigenmanifolds extend eigenspaces to nonlinear mechanical systems with possibly non-Euclidean metrics. Recent work has shown that simple controllers can excite hyper-efficient oscillations by simultaneously stabilizing an Eigenmanifold and regulate the total energy. Yet, existing techniques require imposing assumptions on the system dynamics that the controlled system may not fulfill. This paper overcomes these limitations by allowing for partial dynamic compensation, which produces a good decoupling of the system's dynamics. This decoupling happens in a convenient set of coordinates induced by the modal characterization of the mechanical system. Two control algorithms taking advantage of this property are proposed and validated in simulation.

I. Introduction

The evolution of complex mechanical systems is governed by the interplay of potential fields and dynamic forces. The two actions dynamically balance each other for specific initial conditions, yielding regular oscillations. Often, these oscillations are not isolated but part of entire families continuously evolving from an equilibrium of the system. These collections of periodic orbits are well understood for linear systems thanks to the celebrated linear modal analysis. However, when nonlinearities are involved, the analysis becomes dramatically more complex [1], especially when multi-body effects are involved [2]. Still, most of the interesting oscillatory mechanical systems are nonlinear. For example, animals are well known to rely on natural oscillations to locomote efficiently [3], [4]. Inspired by biology, researchers have introduced elastic and soft elements into the mechanical design of robotic systems, leading to soft robots [5]. These systems are thought to be especially suited for performing oscillatory tasks, and their expected practical applications include locomotion [6], periodic pick and place [7], and carrying payloads that exceed the static torque limits [8]. Elastic elements may also be optimized to maximize performance [9], [10].

Consequently, understanding how to produce nonlinear oscillations in mechanical systems has become an increas-

ingly important goal for control theorists. For example [11]–[13] deal with the challenge from the perspective of virtual holonomic constraints, [14] using immersion and invariance control, [15] through energy shaping, [16] in the context of Floquet theory, and [17] by means of transverse feedback linearization. Alternatives range from optimal control [18], [19] to data-driven methods [20], [21]. Although effective, all these techniques require some form of steady-state dynamic cancellation and persistent excitation.

We focus specifically on exciting oscillatory behaviors that do not require any energy expenditure at a steady state. This is possible only if the desired steady-state orbits are autonomous evolutions of the open-loop system. These oscillations can be identified and described using nonlinear modal theory [2], [22]. Based on this intuition, we recently proposed [23]–[28] to excite nonlinear oscillations by combining two control loops. The first [24] stabilizes nonlinear counterparts of the linear eigenspace: the Eigenmanifolds [2]. The second loop imposes a desired amplitude of oscillations by regulating the total energy of the system [25]. Interestingly, a PD-like regulation of Eigenmanifolds may already be sufficient to realize Eigenmanifold stabilization [24]. Yet, the approach works only under simplifying hypotheses on the transverse dynamics. Even more importantly, to prove the convergence of the nested loops, the energy regulation must be designed not to perturb the invariance of the Eigenmanifold. This is, however, possible only in a restricted class of mechanical systems [25].

The present paper aims to extend this theory to the case in which the model of the system is sufficiently well known to allow for model cancellations during the transient. We show that in this case, the discussed limitations in our framework are overcome by employing a decoupling action. This way, the system can be brought in a special form where a master oscillator acts as a clock for a periodic time-variant system. We propose two controllers - one for Eigenmanifold stabilization and the other for energy regulation - and prove their convergence properties. We then show their effectiveness in exciting the nonlinear modes of a system that we could not have handled using [24], [25].

II. Exciting Efficient Oscillations through Eigenmanifold Stabilization

The formal coordinate-free definition of Eigenmanifold can be found in [2]. We provide here only a brief and coordinate-dependent introduction. We also define here some novel concepts that we will then use to derive the results of

this paper - namely master dynamics, slave variables, and master energy.

A. Dynamics in linear modal coordinates

Consider a generic conservative mechanical system, not subject to non-holonomic constraints, and fully actuated $\ddot{q} = -M^{-1}(q)(C(q,\dot{q})\dot{q}+G(q))+M^{-1}(q)\tau$, where $M(q) \in \mathbb{R}^{n \times n}$ is the inertia matrix, $C(q,\dot{q})\dot{q}$ are Coriolis and centrifugal forces, $G(q)$ are potential forces (usually including gravity and elastic field), and $\tau \in \mathbb{R}^n$ are the generalized forces that we use as inputs. The energy of this system is $E(q,\dot{q}) = \dot{q}^{\mathrm{T}} M(q)\dot{q}/2+U(q)$, with $U(q)$ being the potential energy - i.e. the scalar function having $G(q)$ as gradient vector. Consider now an isolated stable equilibrium q_{eq} of this system. We perform linear modal analysis [2, Sec. II] on the linearized system at the equilibrium. For the sake of space, we suppose that all eigenspaces have dimension two (non resonance condition). We call W the matrix bringing the configuration of the linear system in modal coordinates. Without loss of generality, we order the rows of W such that the first one refers to the eigenspace we aim to extend to the nonlinear realm. To simplify the notation, we introduce the linear change of coordinates $x = W(q - q_{\mathrm{eq}})$, which leads to the dynamics

$$\ddot{x} = f(x,\dot{x}) + g(x)\tau, \tag{1}$$

where $x = [x_1,\ldots,x_n]^{\mathrm{T}} \in \mathbb{R}^n$ are the mechanical system's configuration expressed in the modal coordinates of the linearized system, and $\ddot{x},\dot{x} \in \mathbb{R}^n$ are their time derivatives. The drag of the system is $f : \mathbb{R}^{2n} \to \mathbb{R}^n$, and the input field is the full rank matrix $g : \mathbb{R}^n \to \mathbb{R}^{n \times n}$.

B. Eigenmanifold

Consider system (1) with $\tau = 0$. An Eigenmanifold is a 2-dimensional submanifold of the state space $\mathbb{R}^{2n}$, such that
 i) it contains the equilibrium, i.e. $(0,0) \in \mathfrak{M}$,
 ii) it is a collection of periodic orbits characterized by a distinct energy - i.e. each $x(t)$ such that $(x(0),\dot{x}(0)) \in \mathfrak{M}$ is periodic, it is fully contained in $\mathfrak{M}$, and have a total energy E distinct from all other trajectories in $\mathfrak{M}$,
 iii) all these orbits are line-shaped - i.e. they do not self-intersect, and do not have circular topology.

C. Coordinate embeddings

We say that an Eigenmanifold is an extension of an eigenspace if the latter is tangent to the first at the equilibrium. In the rest of the paper we will focus w.l.o.g. on the Eigenmanifold $\mathfrak{M}$ which is tangent to the eigenspace identified by $(x_1,\dot{x}_1)$. Under this hypothesis we can always introduce (see [2, Secs. 8,9]) two functions $X : \mathbb{R}^2 \to \mathbb{R}^n$ and $\dot{X} : \mathbb{R}^2 \to \mathbb{R}^n$. They are called coordinate embedding of the Eigenmanifold, and they are such that $\mathfrak{M}$ can be defined implicitly as the locus of points that verify

$$x = X(x_1,\dot{x}_1), \quad \dot{x} = \dot{X}(x_1,\dot{x}_1). \tag{2}$$

Note for (2) to be verified $(X_1,\dot{X}_1)$ must be the identity function. We will release in the next future a tool for automatically evaluate $X,\dot{X}$ from (1).
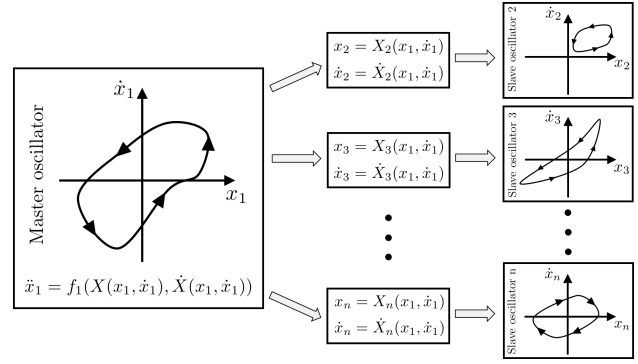

Fig. 1. If initialized on the invariant manifold, the system's evolution is entirely defined by the one-dimensional dynamics of the master variable. The remaining $n-1$ slave variables are specified by the master variable through a set of nonlinear algebraic functions.

D. Master dynamics and slave variables

We call modal dynamics the following second order system

$$\ddot{x}_1 = f_1(X(x_1,\dot{x}_1), \dot{X}(x_1,\dot{x}_1)) \tag{3}$$

When evolving on the Eigenmanifold system (1) behaves as the 1-DoF system (3), and all the other variables are constrained by the algebraic rules (2). For this reason, we refer to $(x_1,\dot{x}_1)$ as master variables and the remaining part of the state as slave variables. Note that this is a standard terminology that we are borrowing from [29]. Fig. 1 depicts this idea. This structure is lost as soon as we leave the manifold, even if in the immediate boundary.

Finally, we define the energy of the master dynamics as

$$E_{\mathfrak{M}} = E(X(x_1,\dot{x}_1), X(x_1,\dot{x}_1)), \tag{4}$$

from which it is clear that in the general case (3) is not itself a mechanical system. For example, the energy is in not quadratic in $\dot{x}_1$ as soon as $\dot{X}$ is not linear in $\dot{x}_1$.

E. Tangency constraints

Since the Eigenmanifold is invariant by definition, time derivative of the state $(\dot{x}_1, \ddot{x}_1)$ must always be tangent to the Eigenmanifold itself (i.e. zero orthogonal component). A simple way to express this condition is to evaluate the time derivative of (2), and then substitute the vector field (1). We then substitute back $x = X(x_1,\dot{x}_1)$ and $\dot{x} = \dot{X}(x_1,\dot{x}_1)$. This process yields the tangency constraints

$$\dot{X}_j = \frac{\partial X_j}{\partial x_1}\dot{x}_1 + \frac{\partial X_j}{\partial \dot{x}_1}f_1(X(x_1,\dot{x}_1), \dot{X}(x_1,\dot{x}_1)),$$
$$f_j(X,\dot{X}) = \frac{\partial \dot{X}_j}{\partial x_1}\dot{x}_1 + \frac{\partial \dot{X}_j}{\partial \dot{x}_1}f_1(X(x_1,\dot{x}_1), \dot{X}(x_1,\dot{x}_1)). \tag{5}$$

$\forall j \in \{2\ldots n\}$. Note that $j = 1$ trivially holds. The master dynamics (3) clearly assumes an important role here.

III. EIGENMANIFOLD STABILIZATION

This section introduces a new feedback controller, whose aim is to make the Eigenmanifold $\mathfrak{M}$ a local attractor for the closed-loop system. We have already shown in [24] that achieving such a goal results in the generation of
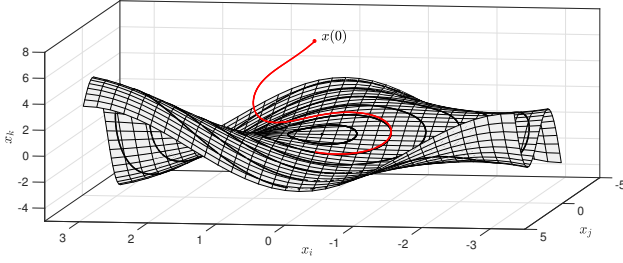
Fig. 2. Making the Eigenmanifold $\mathfrak{M}$ an attractor using feedback control is a simple way of generating regular steady-state oscillations that do not need any persistent excitation to be sustained at steady-state. This is because they are already open-loop evolutions of the system. Yet, an Eigenmanifold contains infinite modal oscillations - some of which are shown in the picture as solid lines. Since a different energy level labels each mode, we can pick the desired one by including a further feedback action that regulates the energy of the mechanical system.

nonlinear oscillations that require no persistent excitation to be sustained. This idea is summarized by Fig. 2. Yet, the simple PD-like action proposed in our previous work only worked under simplifying assumptions.

We have seen in Sec. II-D and Fig. 1 that the system assumes a simplified structure when evolving on the Eigenmanifold. We aim here to design a feedback action that can force similar hierarchical dynamics in the vicinity of the Eigenmanifold. We propose to achieve this goal through compensatory acceleration acting only on the master variable

$$a_1(x, \dot{x}) = f_1(X(x_1, \dot{x}_1), \dot{X}(x_1, \dot{x}_1)) - f_1(x, \dot{x}), \quad (6)$$

which in turn can be used to augment a PD-like loop

$$\tau(x, \dot{x}) = g^{-1}(x) \left(\kappa_{\mathrm{p}} \Delta + \kappa_{\mathrm{d}} \dot{\Delta} + \begin{bmatrix} a_1(x, \dot{x}) \\ 0 \\ \vdots \\ 0 \end{bmatrix} \right), \quad (7)$$

where $\kappa_{\mathrm{p}} \in \mathbb{R}^+$, $\kappa_{\mathrm{d}} \in \mathbb{R}^+$, $\Delta = X(x_1, \dot{x}_1) - x$, and $\dot{\Delta}$ is the time derivative of Δ.

Lemma 1. *If* (8) *is asymptotically stable with* $(\xi, \dot{\xi})$ *open loop evolution of* $\ddot{\xi} = f_1(X(\xi, \dot{\xi}), \dot{X}(\xi, \dot{\xi}))$, *then* (7) *makes* $\mathfrak{M}$ *a local attractor of the closed loop system.*

Proof. Differentiating w.r.t. time $\Delta_j = X_j(x_1, \dot{x}_1) - x_j$ yields

$$\begin{aligned} \dot{\Delta}_j &= -\dot{x}_j + \frac{\partial X_j}{\partial x_1} \dot{x}_1 + \frac{\partial X_j}{\partial \dot{x}_1}[f_1(x, \dot{x}) + g_1(x)\tau] \\ &= -\dot{x}_j + \dot{X}_j(x_1, \dot{x}_1) \\ &\quad + \frac{\partial X_j}{\partial \dot{x}_1}[f_1(x, \dot{x}) - f_1(X, \dot{X}) + g_1(x)\tau] , \end{aligned}$$

where in the first step we used the chain rule, and in the second step we used (5), i.e. the manifold invariance. Now, we close the loop with (7) and (6). Recalling that $\Delta_1 \equiv 0$ by definition yields

$$\dot{\Delta}_j = \dot{X}_j(x_1, \dot{x}_1) - \dot{x}_j , \quad (9)$$

which now describes the displacement between velocities and corresponding manifold coordinates. We differentiate (9) a second time obtaining

$$\begin{aligned} \ddot{\Delta}_j &= - f_j(x, \dot{x}) - g_j(x)\tau_j \\ &\quad + \frac{\partial \dot{X}_j}{\partial x_1} \dot{x}_1 + \frac{\partial \dot{X}_j}{\partial \dot{x}_1}[f_1(x, \dot{x}) + a_1] \\ &= - f_j(x, \dot{x}) - g_j(x)\tau_j \\ &\quad + \frac{\partial \dot{X}_j}{\partial x_1} \dot{x}_1 + \frac{\partial \dot{X}_j}{\partial \dot{x}_1} f_1(X(x_1, \dot{x}_1), \dot{X}(x_1, \dot{x}_1)) , \end{aligned} \quad (10)$$

where again we applied the chain rule and plugged in (6) and (7). Now, we exploit once more the tangency constraints (5), together with the definition of Δ and the expression of its time derivative (9). The result is

$$\ddot{\Delta}_j = f_j(X, \dot{X}) - f_j(X - \Delta, \dot{X} - \dot{\Delta}) - \kappa_{\mathrm{p}} \Delta_j - \kappa_{\mathrm{d}} \dot{\Delta}_j .$$

To complete the proof, we linearize the dynamics for small displacements from the manifold $\mathfrak{M}$, i.e. around $\Delta_j = 0$ and $\dot{\Delta}_j = 0 \ \forall j \in \{2 \ldots n\}$. The result is (8), with $z = \begin{bmatrix} \Delta_2 \ldots \Delta_n \end{bmatrix}^{\mathrm{T}}$ and $\dot{z} = \begin{bmatrix} \dot{\Delta}_2 \ldots \dot{\Delta}_n \end{bmatrix}^{\mathrm{T}}$, and where we exploited that $\Delta_1 \equiv 0$ and $\dot{\Delta}_1 \equiv 0$ by construction. In (8), x_1 and $\dot{x}_1$ do not appear as an input, but only as dependencies in the dynamic matrix. Indeed, the following equations hold

$$\frac{\partial f_j(x, \dot{x})}{\partial x_1} = \left. \frac{\partial f_j(X - \Delta, \dot{X} - \dot{\Delta})}{\partial x_1} \right|_{\substack{\Delta_j = 0 \\ \dot{\Delta}_j = 0}} , \quad (11)$$

$$\frac{\partial f_j(x, \dot{x})}{\partial \dot{x}_1} = \left. \frac{\partial f_j(X - \Delta, \dot{X} - \dot{\Delta})}{\partial \dot{x}_1} \right|_{\substack{\Delta_j = 0 \\ \dot{\Delta}_j = 0}} . \quad (12)$$

Note that the controller a_1 decouples the dynamics of master variable from the slave variables. Indeed it holds $\ddot{x}_1 = f_1(x, \dot{x}) + (f_1(X(x_1, \dot{x}_1), \dot{X}(x_1, \dot{x}_1)) - f_1(x, \dot{x})) = f_1(X(x_1, \dot{x}_1), \dot{X}(x_1, \dot{x}_1))$, i.e. x_1 evolves according to the modal dynamics (3) also outside the manifold. Thus, the dependency of (8) from ξ and $\dot{\xi}$ can be regarded as a time-variance. $\square$

IV. ENERGY REGULATION

The advantages of introducing the decoupling action (6) do not stop the challenge of making the Eigenmanifold a local attractor. On the contrary, we can leverage the simplified resulting dynamics to include an energy regulation loop and still prove convergence to the desired behavior. Achieving this goal without (6) requires imposing strong constraints to the kind of behaviors that can be implemented and to the control actions that must be exerted - as discussed in [25]. Also, it would require to be able to regulate the displacements from the Eigenmanifold in finite time. Note that regulating the energy is paramount in our framework since it allows to select of the desired oscillation among the infinite similar ones which are part of the same Eigenmanifold (see Fig. 2). This, in practice, means selecting the amplitude of the oscillation.

We propose to inject or remove energy from the system when needed with a simple bang-bang loop (14), which accelerates the master variable only. The modal energy $E_{\mathfrak{M}}$

2450

$$\dot{z} = \begin{bmatrix} 0 & I \\ -\Sigma(\xi(t),\dot{\xi}(t)) - \kappa_{\mathrm{p}} & -\Gamma(\xi(t),\dot{\xi}(t)) - \kappa_{\mathrm{d}} \end{bmatrix} z, \quad \text{with } \Sigma_{i,j}(x_1,\dot{x}_1) = \left.\frac{\partial f_{i+1}}{\partial x_{j+1}}\right|_{\substack{x=X,\\ \dot{x}=\dot{X}}}, \quad \Gamma_{i,j}(x_1,\dot{x}_1) = \left.\frac{\partial f_{i+1}}{\partial \dot{x}_{j+1}}\right|_{\substack{x=X,\\ \dot{x}=\dot{X}}}. \qquad (8)$$

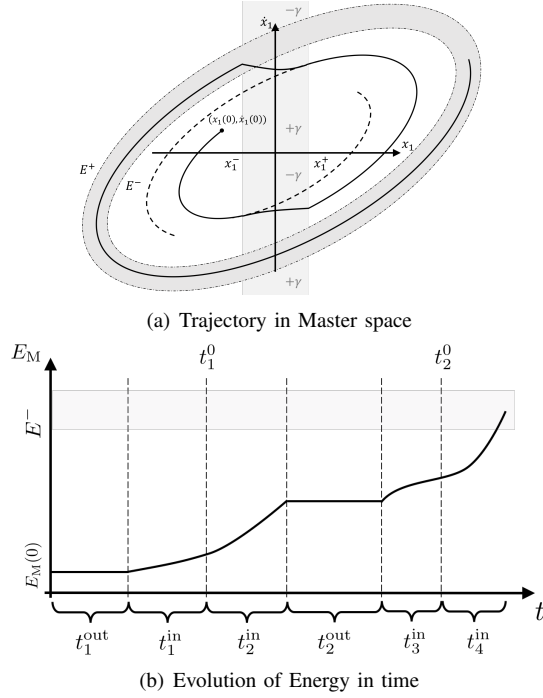(a) Trajectory in Master space

(b) Evolution of Energy in time

Fig. 3. Pictorial example of the effect of (13). Panel (a) presents an evolution in master variables space $(x_1, \dot{x}_1)$, while Panel (b) presents the corresponding evolution of the energy in time. When the system is in a neighborhood of equilibrium configuration $x_1 = 0$ (i.e., when it crosses the gray area), energy is injected by the controller, moving the system to another of its autonomous orbits. Eventually, this brings the robot to the region of state space with the desired amount of energy. labelfig:bangbang

is defined in (4). The key idea here is that thanks to discussed decoupling operated by (6) we can look at the master dynamics as a conservative autonomous system. Thus we can regulate the modal energy and then wait that E converges to $E_{\mathfrak{M}}$ when the system reaches the Eigenmanifold.

Thus, combining (14) with the controller (7) yields

$$\tau(x,\dot{x}) = g^{-1}(x) \left(\kappa_{\mathrm{p}} \, \Delta + \kappa_{\mathrm{d}} \, \dot{\Delta} + \begin{bmatrix} a_1(x,\dot{x}) + \bar{a}_1(x_1,\dot{x}_1) \\ 0 \\ \vdots \\ 0 \end{bmatrix} \right), \tag{13}$$

where $\gamma > 0$, $E^+ > E^- > 0$, and $x_1^+ > 0 > x_1^-$ are scalar constants. a_1 is the decoupling action (6).

Lemma 2. *If the following hypotheses hold*

H1 *the level curves of the modal energy $E_{\mathfrak{M}}$ are closed*
H2 $f_1(X(x_1,0), \dot{X}(x_1,0)) \notin \{0,\gamma\} \ \forall x_1 \notin [x_1^-, x_1^+]$
H3 *the hypotheses of Theorem 1 are verified*

then (13) produces a closed loop system having $\mathfrak{M}$ as a local attractor and $\lim_{t\to\infty} E(x(t),\dot{x}(t)) \in [E^-, E^+]$.

Proof. We consider the case $E(x_1(0),\dot{x}_1(0)) < E^-$, which we sketch in Fig. **??**. The proof for $E(x_1(0),\dot{x}_1(0)) > E^+$

follows similar arguments. Thus, the closed loop dynamics of the master variable x_1 is

$$\ddot{x}_1 = f_1(X(x_1,\dot{x}_1), \dot{X}(x_1,\dot{x}_1))$$
$$+ \begin{cases} 0 & \text{if } x_1 \notin [x_1^-, x_1^+] \\ + \gamma & \text{if } x_1 \in [x_1^-, x_1^+] \wedge \dot{x}_1 > 0 \\ - \gamma & \text{otherwise,} \end{cases} \tag{15}$$

which is autonomous, and it does not depend on the evolution of slave variables $x_2 \ldots x_n$. Note that system (15) verifies the basic conditions [30, Sec. 2.7]. Thus, its solution always exists unique and finite for a given initial condition.

a) Time partitioning: We introduce a partition of the time into a sequence of intervals [31]

$$[0,t) = (\bigcup_1^{i^+(t)} t_i^{\mathrm{in}}) \cup (\bigcup_1^{j^+(t)} t_j^{\mathrm{out}}) \cup (\bigcup_1^{k^+(t)} t_k^0), \tag{16}$$

where (a) t_i^{in} is the $i-th$ interval for which $x_1 \in [x_1^-, x_1^+]$ and $\dot{x}_1 \neq 0$; (b) t_j^{out} is the $j-th$ interval for which $x_1 \notin [x_1^-, x_1^+]$; (c) t_k^0 is the $k-th$ interval for which $x_1 \in [x_1^-, x_1^+]$ and $\dot{x}_1 = 0$. $i^+(t), j^+(t), k^+(t)$ are the number of intervals $t_i^{\mathrm{in}}, t_j^{\mathrm{out}}, t_k^0$ contained in $[0,t)$. Of the three classes of intervals, only in t_i^{in} energy is introduced in the system.

b) The system always exits from $x_1(t) \notin [x_1^-, x_1^+]$: If $x_1(t) \notin [x_1^-, x_1^+]$ then (15) becomes $\ddot{x}_1 = f_1(X(x_1,\dot{x}_1), \dot{X}(x_1,\dot{x}_1))$, which is the master variable's dynamics on the manifold (3).

Since the system is conservative, then the modal energy is constant in time. As a consequence

$$\frac{\mathrm{d}E_{\mathfrak{M}}}{\mathrm{d}t} = 0 \Rightarrow \frac{\mathrm{d}E_{\mathfrak{M}}}{\mathrm{d}x_1}\dot{x}_1 + \frac{\mathrm{d}E_{\mathfrak{M}}}{\mathrm{d}\dot{x}_1}\ddot{x}_1 = 0, \tag{17}$$

i.e. x_1 evolves on the level curves of $E_{\mathfrak{M}}$. Note that this is not a trivial consequence of the conservation of energy, but it also required that modal energy is dependent only from the master variables. This property, together with H1, implies that the orbits $(x_1, \dot{x}_1)$ intercept the interval $[x_1^-, x_1^+]$. Finally, H2 assures that (3) has no equilibrium on the orbit. This is sufficient to that the evolution of x_1 reaches the interval $[x_1^-, x_1^+]$ in finite time. So each t_j^{out} is finite, and it is always followed by a t_i^{in}.

c) Energy increases in t_i^{in}: When $x_1 \in [x_1^-, x_1^+]$ and $\dot{x}_1 \neq 0$, (15) is excited by a nonconservative force. This implies a energy change equal to

$$\frac{\mathrm{d}E_{\mathfrak{M}}}{\mathrm{d}t}(x_1,\dot{x}_1) = \dot{x}_1 \begin{cases} +\gamma & \text{if } \dot{x}_1 > 0 \\ -\gamma & \text{otherwise} \end{cases} \tag{18}$$
$$= \gamma |\dot{x}_1| > 0, \qquad \forall t \in t_i^{\mathrm{in}}.$$

d) Energy increases in time: Conditions $x_1 \in [x_1^-, x_1^+]$ and $\dot{x}_1 = 0$ hold only for isolated instants, since H3 implies $\ddot{x}_1 \neq 0$. Thus t_k^0 are all of zero measure. Putting together

$$\bar{a}_1 = \gamma \begin{cases} 0 & \text{if } x_1 \notin [x_1^-, x_1^+] \text{ or } E_{\mathfrak{M}} \in [E^-, E^+] \\ 1 & \text{if } x_1 \in [x_1^-, x_1^+] \text{ and } ((E_{\mathfrak{M}} < E^- \text{ and } \dot{x}_1 > 0) \text{ or } (E_{\mathfrak{M}} > E^+ \text{ and } \dot{x}_1 < 0)) \\ -1 & \text{otherwise.} \end{cases} \quad (14)$$
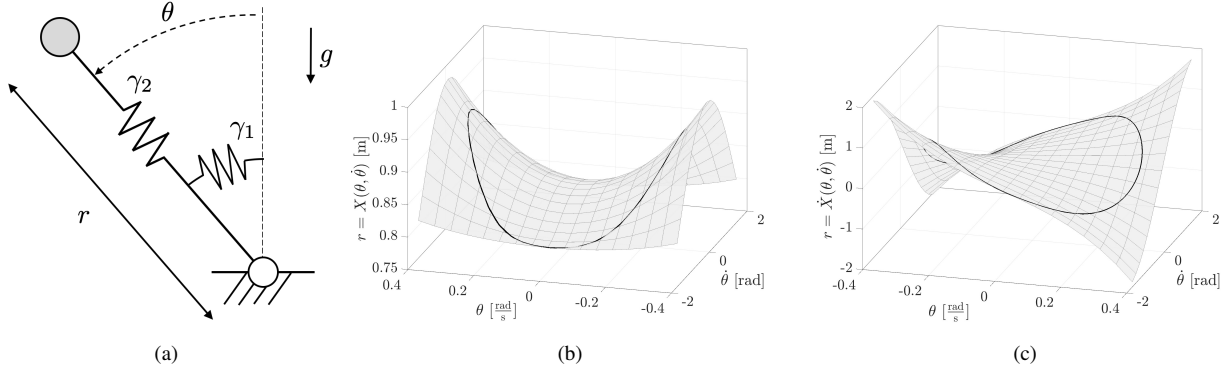

Fig. 4. Panel (a) shows the generalized inverted elastic pendulum, with main quantities underlined. θ and r are the polar coordinates of the point mass. γ_1 and γ_2 are a polar and a radial spring, normalized by the mass. γ_1 is equal to zero in the classic inverted elastic pendulum model. The mass is subjected to a constant gravitational field g. Panels (b) and (c) show the Eigenmanifold of system (20), for $\gamma_1 = 20 \frac{1}{s^2}$, $\gamma_2 = 60 \frac{1}{s^2}$, $g = 9.81 \frac{m}{s^2}$, $r_0 = 1$m. The solid line is the trajectory corresponding to the initial condition $\theta = 0$ and $\dot{\theta} = \frac{\pi}{2} \frac{rad}{s}$.
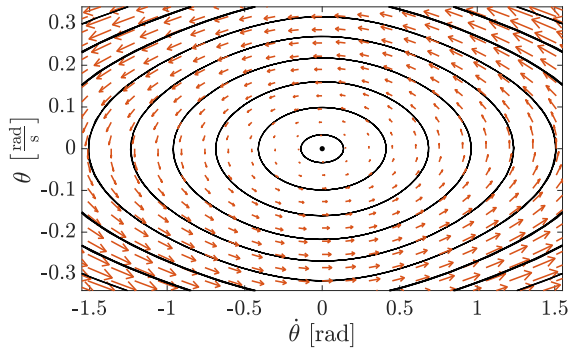

Fig. 5. Representation of the modal dynamics of the generalized inverted pendulum. The red arrows are a representation of the modal acceleration field $f_1(X, \dot{X})$. The black lines are examples of modal oscillations expressed in modal coordinates.

the energy balances for all the intervals yields

$$\begin{aligned} E_{\mathfrak{M}}(t) &= E_{\mathfrak{M}}(0) + \int_0^t \frac{dE_{\mathfrak{M}}}{dt} \, dt' \\ &= E_{\mathfrak{M}}(0) + \int_0^{\bar{t}} \frac{dE_{\mathfrak{M}}}{dt} \, dt'' \\ &\geq E_{\mathfrak{M}}(0) + \epsilon\bar{t}, \end{aligned} \quad (19)$$

where $\bar{t} = \sum_1^{i^+(t)} \max(t_i^{in})$, and in the second step we changed the integral coordinate to express the time as union of t_i^{in} intervals.

e) $E_{\mathfrak{M}}$ reaches $[E^-, E^+]$ in finite time: Eqs. (18) and (19) imply that $E_{\mathfrak{M}}(t)$ is increasing for $E_{\mathfrak{M}} < E^-$. Thus x_1 and $\dot{x}_1$ eventually reach a value such that $E_{\mathfrak{M}} = E^-$. Since (17), then once reached the desired energy band $[E^-, E^+]$, the model energy $E_{\mathfrak{M}}$ remains in it. Therefore a $T \in \mathbb{R}$ always exists such that $E_{\mathfrak{M}}(x_1(t), \dot{x}_1(t)) \in [E^-, E^+]$ for all the $t > T$.

f) E reaches $[E^-, E^+]$ asymptotically: The previous step of the proof implies that $\bar{a}_1(x_1(t), \dot{x}_1(t)) = 0$, and (13) is equal to (7) for all the $t > T$. The manifold attractiveness follows from H3 and lemma 1, and in turn

$$\lim_{t \to \infty} E(x(t), \dot{x}(t)) = \lim_{t \to \infty} E_{\mathfrak{M}}(x_1(t), \dot{x}_1(t)) \in [E^-, E^+] .$$

$\square$

It is worth mentioning that both controllers (7) and (13) are such that $\tau_i \to 0$, since $\tau_i(x_1, \dot{x}_1, X_2, \dot{X}_2, \ldots, X_n, \dot{X}_n) \equiv 0$. So the closed loop system evolves autonomously at steady state, without any injection of external energy. Also, note that E^- and E^+ can be selected arbitrarily close to each other. However, smaller is the interval $[E^-, E^+]$ higher are the chances of chattering in the practice.

V. SIMULATION

We present here the application of the proposed strategy to a representative yet straightforward example of a nonlinear mechanical system: the generalized inverted elastic pendulum shown in Fig. 4(a). Note that the controllers that we have proposed in our previous work [25] cannot be applied to this system since its Eigenmanifold does not self-intersects when projected in configuration space - as we will see later in this section.

The system's dynamics is

$$\begin{aligned} \ddot{\theta} &= -2\frac{\dot{r}}{r}\dot{\theta} + \frac{g}{r}\sin(\theta) - \frac{\gamma_1}{r^2}\theta + \frac{\tau_\theta}{m}, \\ \ddot{r} &= +r\dot{\theta}^2 - g\cos(\theta) - \gamma_2(r - r_0) + \frac{\tau_r}{m} , \end{aligned} \quad (20)$$

where θ and r are the polar coordinates of the body, with their derivatives $\dot{\theta}$, $\ddot{\theta}$, $\dot{r}$, $\ddot{r}$. g is the gravity constant. γ_1 and γ_2 are the ratio between stiffnesses of both springs and the body mass m. The system has an equilibrium in $\theta \equiv 0$ and
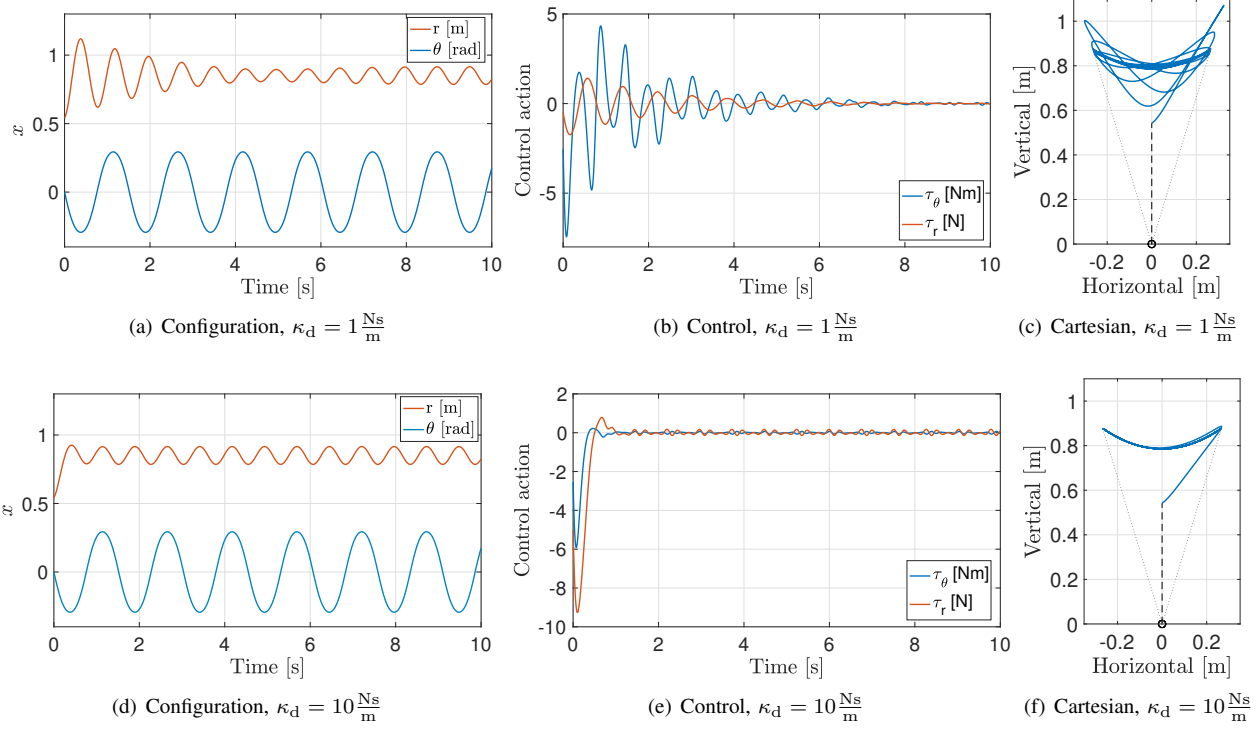
2452

(a) Configuration, $\kappa_\mathrm{d} = 1\frac{\mathrm{Ns}}{\mathrm{m}}$
(b) Control, $\kappa_\mathrm{d} = 1\frac{\mathrm{Ns}}{\mathrm{m}}$
(c) Cartesian, $\kappa_\mathrm{d} = 1\frac{\mathrm{Ns}}{\mathrm{m}}$
(d) Configuration, $\kappa_\mathrm{d} = 10\frac{\mathrm{Ns}}{\mathrm{m}}$
(e) Control, $\kappa_\mathrm{d} = 10\frac{\mathrm{Ns}}{\mathrm{m}}$
(f) Cartesian, $\kappa_\mathrm{d} = 10\frac{\mathrm{Ns}}{\mathrm{m}}$

Fig. 6. Inverted elastic pendulum (20) controlled through (7), with $\kappa_\mathrm{d} = 1\frac{\mathrm{Ns}}{\mathrm{m}}$ (a,b,c), $\kappa_\mathrm{d} = 10\frac{\mathrm{Ns}}{\mathrm{m}}$ (d,e,f). The considered physical parameters are $\gamma_1 = 20\frac{1}{\mathrm{s}^2}$, $\gamma_2 = 60\frac{1}{\mathrm{s}^2}$, $g = 9.81\frac{\mathrm{m}}{\mathrm{s}^2}$, $r_0 = 1$m. The selected initial condition is $\theta = 0$, $\dot{\theta} = \frac{7}{16}\pi\frac{\mathrm{rad}}{\mathrm{s}}$, $r \simeq 0.54$m, $\dot{r} = 0.5\frac{\mathrm{m}}{\mathrm{s}}$. Note that for these values the system is outside the invariant manifold, indeed $r(0) - X(\theta(0),\dot{\theta}(0)) \simeq -\frac{1}{4}$m and $\dot{r}(0) - \dot{X}(\theta(0),\dot{\theta}(0)) = -0.5\frac{\mathrm{m}}{\mathrm{s}}$. Panels (a,d) present the time evolution of the Lagrangian variables θ and r. Panels (b,e) show the control action generated by the controller. Panels (c,f) present the evolution of the mass in Cartesian space.

$r \equiv r_0 - \frac{g}{\gamma_2}$. Its linearized dynamics is

$$\Delta\ddot{\theta} \simeq \left(\frac{g(r_0 - \frac{g}{\gamma_2}) - \gamma_1}{(r_0 - \frac{g}{\gamma_2})^2}\right)\Delta\theta, \quad \Delta\ddot{r} \simeq -\gamma_2\Delta r. \quad (21)$$

So, the normal modes of the linearized system are two decoupled evolutions: an angular oscillation with fixed radius, and a radial oscillation with fixed angle. The nonlinear extension of the latter is trivial, since for $\theta \equiv 0$ and $\dot{\theta} \equiv 0$ the dynamics collapses into a linear one.

The other mode turns into a more complex oscillation, characterized by a non strict Eigenmanifold. We evaluate its parametrization $(X, \dot{X})$ by approximating the solution of (5) extending a Galerkin procedure tipically used in center manifold theory [29]. We approximate (20) with a 3rd order Taylor expansion around the equilibrium. We then consider the symmetry of (20), w.r.t. θ and around $\theta = 0$. If $(\hat{\theta}, \dot{\hat{\theta}}, \hat{r}, \dot{\hat{r}})$ is a system evolution, than also $(-\hat{\theta}, -\dot{\hat{\theta}}, \hat{r}, \dot{\hat{r}})$ is. This implies that X and $\dot{X}$ must be even. Therefore, we consider as guess for the two maps a fourth order polynomial without odd terms. This implicitly assures that the tangent to the Eigenmanifold at the equilibrium is the linear eigenspace. We force condition (i) to hold by taking the constant terms of the polynomial to be the equilibrium of the system. Plugging the Taylor approximation of the dynamics and the polinomial guesses for $X, \dot{X}$ into (5) yields 12 algebraic equations in the parameters of the polynomial. We cannot report them here for the sake of space. We used *solve*

function from `MatLab` to solve them. Substituting the two maps into the dynamics of θ, we obtain the modal dynamics $\ddot{\theta} = -2\frac{\dot{X}_2(\theta,\dot{\theta})}{X_2(\theta,\dot{\theta})}\dot{\theta} + \frac{g\,X_2(\theta,\dot{\theta})\sin(\theta) - \gamma_1\,\theta}{X_2(\theta,\dot{\theta})^2}$. As an example, we take $\gamma_1 = 20\frac{1}{\mathrm{s}^2}$ and $\gamma_2 = 60\frac{1}{\mathrm{s}^2}$. Figs. 4(b) and 4(c) show the resulting Eigenmanifold. The orbit corresponding to the initial condition $\theta = 0$ and $\dot{\theta} = \frac{\pi}{2}\frac{\mathrm{rad}}{\mathrm{s}}$ is superimposed as an example. Fig. 5 depicts the resulting modal dynamics.

We consider now the application of the control law (7) to make the Eigenmanifold parametrized by X and $\dot{X}$ an attractor. Σ and Γ are the scalars $\Sigma = -\gamma_2 + \dot{\theta}^2$, $\Gamma = 0$. Thus, the stability of the transverse dynamics (8) is proven using [32], which yields $\gamma_2 + \kappa_\mathrm{p} > \dot{\theta}^2$ and $\kappa_\mathrm{d} > \frac{2\dot{\theta}\ddot{\theta}}{\dot{\theta}^2 - \gamma_2}$. So, in case the speed of the master variable is not too big compared to the radial stiffness, a pure damping feedback on r is sufficient to make the Eigenmanifold an attractor. Fig. 6 presents the evolution of the system (20) controlled through (7). We present two different choices of κ_d: low gain $1\frac{\mathrm{Ns}}{\mathrm{m}}$, and higher gain $\kappa_\mathrm{d} = 10\frac{\mathrm{Ns}}{\mathrm{m}}$. The initial condition is $\theta = 0$, $\dot{\theta} = \frac{7}{16}\pi\frac{\mathrm{rad}}{\mathrm{s}}$, $r = X(0,\frac{7}{16}\pi) - \frac{1}{4}$m $\simeq 0.54$m, $\dot{r} = \dot{X}(0,\frac{7}{16}\pi) - 0.5\frac{\mathrm{m}}{\mathrm{s}} = 0.5\frac{\mathrm{m}}{\mathrm{s}}$. In both cases the robot converges to a stable oscillation. Panels (a,d) show the time evolutions. In the less damped case (a-c), r takes more time to converge, and does that with an overshoot. Looking to the control actions (b,e), this translates into a more prominent action of the decoupling controller τ_θ. Note that in both cases the control action converges to values close to zero, i.e. the robot evolves on the manifold following autonomous
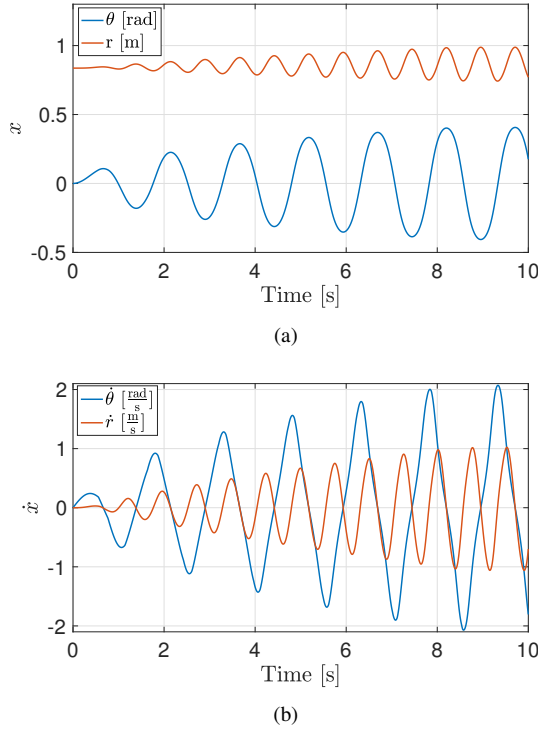
(a)

(b)

Fig. 7. Evolution of inverted elastic pendulum (20) controlled through (13), with $\kappa_d = 10\frac{\mathrm{Ns}}{\mathrm{m}}$, $E^- = 21\mathrm{J}$, $E^+ = 22\mathrm{J}$, $x^- = -\frac{\pi}{32}$, $x^+ = +\frac{\pi}{32}$, $\gamma = 1\mathrm{N}$. The system starts from the equilibrium $r = r_0 - \frac{g}{\kappa_1}$, $\theta = 0$. The controller successfully increases the system oscillations, while maintaining the two degrees of freedom synchronized (i.e. on the modal manifold). This is particularly evident in panel (b).

trajectories. The small deviations from the null value are due to the mismatches between ideal and approximated maps $X, \dot{X}$. Panels (c,f) show the trajectory of the center of mass in Cartesian space. A much more dynamic transient can be observed in (c).

Fig. 7 presents the time evolutions of system (20) controlled through the complete controller (13). Note that the system is conservative, and the energy $E(\theta, \dot{\theta}, r, \dot{r}) = \frac{1}{2}(r^2\dot{\theta}^2 + \dot{r}^2) + \frac{1}{2}(\gamma_1\theta^2 + \kappa_2(r - r_0)^2) + g(r\cos(\theta))$ has closed level curves, thus fulfilling the hypotheses of lemma 2. We considered $E^- = 21\mathrm{J}$, $E^+ = 22\mathrm{J}$, $x^- = -\frac{\pi}{32}$, $x^+ = +\frac{\pi}{32}$, $\gamma = 1\mathrm{N}$. The system starts at the equilibrium, i.e. $\theta = 0$, $r = r_0 - \frac{g}{\kappa_2} \simeq 0.84\mathrm{m}$, $\dot{\theta} = 0$, $\dot{r} = 0$, and it reaches the desired level of energy after about 9s. Note that thanks to the stabilizing controller, evolutions remain synchronized during the whole excitation phase despite the perturbations. This is evident from the zero-crossings of the velocity in Fig. 7 (b). The same figure also highlights a key characteristics of the considered mode: the frequency of oscillation of θ is half of the frequency of oscillation of r. This type of non-unison oscillations are a peculiar product of the non-linear dynamics, made possible by the fact that the parametrization of the manifold X decreases in one direction and increases in the other (see Fig. 4(b)). For the same simulation, Fig. 8(a) presents the Cartesian evolution of the center of mass. Fig. 8(b) reports a comparison between the control actions

exerted by the proposed controller (τ_θ and τ_r), and the ones that would have been necessary to regulate an equivalent rigid robot along the same trajectory when the mass is 1Kg ($\tau_{\theta,\mathrm{fa}}$ and $\tau_{r,\mathrm{fa}}$). Fig. 8(c) shows the trajectory in (a portion of) state space, which can be qualitatively compared with Fig. 4(b). Finally, in Fig. 9 we report the application of the proposed control strategies to a more complex system: a 3-DoF planar manipulator. Due to space limitations, we cannot show the derivation of the Eigenmanifold embedding and the associated control rule, which follows the same steps as for the generalized elastic pendulum discussed above. This example is meant to show the generality of the method.

VI. CONCLUSIONS

This paper proposed a model-based solution to the problem of exciting nonlinear oscillations through Eigenmanifold stabilization and energy injection. This solution can be used when a good knowledge of the master variable dynamics is available. We showed that by including a model-based compensation in our control strategy, the transverse dynamics could be studied locally as a linear problem, and the energy regulation can be achieved in finite time through a bang-bang controller. Future work will be devoted to assessing global convergence, including a more robust mechanism to compensate for energy losses and validating the results experimentally on a multi-DoF robotic system. Furthermore, we will release a toolbox for automatically evaluating the expression of $X, \dot{X}$ of a given mechanical system.

REFERENCES

[1] G. Kerschen, M. Peeters, J.-C. Golinval, and A. F. Vakakis, "Nonlinear normal modes, part i: A useful framework for the structural dynamicist," *Mechanical Systems and Signal Processing*, vol. 23, no. 1, pp. 170–194, 2009.

[2] A. Albu-Schaeffer and C. Della Santina, "A review on nonlinear modes in conservative mechanical systems," *Annual Reviews in Control*, 2020.

[3] H. Geyer, A. Seyfarth, and R. Blickhan, "Compliant leg behaviour explains basic dynamics of walking and running," *Proceedings of the Royal Society B: Biological Sciences*, vol. 273, no. 1603, pp. 2861–2867, 2006.

[4] Ö. Drama and A. Badri-Spröwitz, "Trunk pitch oscillations for energy trade-offs in bipedal running birds and robots," *Bioinspiration & biomimetics*, vol. 15, no. 3, p. 036013, 2020.

[5] C. Della Santina, M. G. Catalano, and A. Bicchi, "Soft robots," in *Encyclopedia of Robotics*, M. Ang, O. Khatib, and B. Siciliano, Eds. Springer, 2020.

[6] M. Calisti, G. Picardi, and C. Laschi, "Fundamentals of soft robot locomotion," *Journal of The Royal Society Interface*, vol. 14, no. 130, p. 20170101, 2017.

[7] L. B. Bonacchi, M. A. Roa, A. Sesselmann, F. Loeffl, A. Albu-Schaffer, and C. Della Santina, "Efficient and goal-directed oscillations in articulated soft robots: the point-to-point case," *IEEE Robotics and Automation Letters*, 2021.

[8] R. B. Hill, S. Briot, A. Chriette, and P. Martinet, "Exploiting natural dynamics in order to increase the feasible static-wrench workspace of robots," in *IFToMM World Congress on Mechanism and Machine Science*. Springer, 2019, pp. 2169–2178.

[9] L. F. Van Der Spaa, W. J. Wolfslag, and M. Wisse, "Unparameterized optimization of the spring characteristic of parallel elastic actuators," *IEEE Robotics and Automation Letters*, vol. 4, no. 2, pp. 854–861, 2019.

[10] W. Roozing, Z. Ren, and N. G. Tsagarakis, "An efficient leg with series–parallel and biarticular compliant actuation: design optimization, modeling, and control of the eleg," *The International Journal of Robotics Research*, p. 0278364919893762.
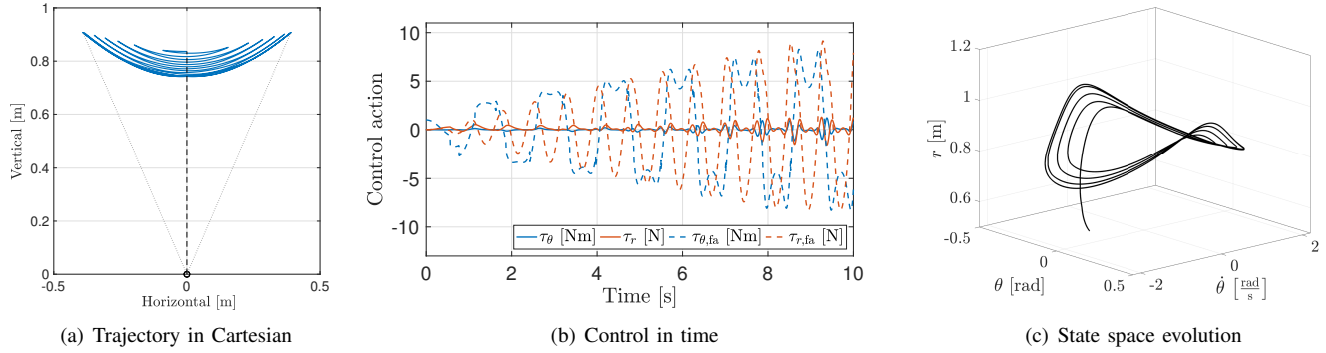
(a) Trajectory in Cartesian
(b) Control in time
(c) State space evolution

Fig. 8. Panel (a) shows the Cartesian evolution of inverted elastic pendulum (20) controlled through (13). We select the parameters $\kappa_d = 10$, $E^- = 21J$, $E^+ = 22J$, $x^- = -\frac{\pi}{32}$, $x^+ = +\frac{\pi}{32}$, $\gamma = 1N$. The system starts from the equilibrium $r = r_0 - \frac{g}{\kappa_1}$, $\theta = 0$. Note that only the transient is shown here. In Panel (b) the control actions generated by the controller are presented in solid line. The dashed lines indicate the actions that would have been needed to implement the same behavior in a rigid system through a standard computed torque algorithm. Panel (c) shows the evolution in state space ($\dot{r}$ not shown). The trajectory asymptotically converge to an hyper efficient regular oscillation with the desired energy level.
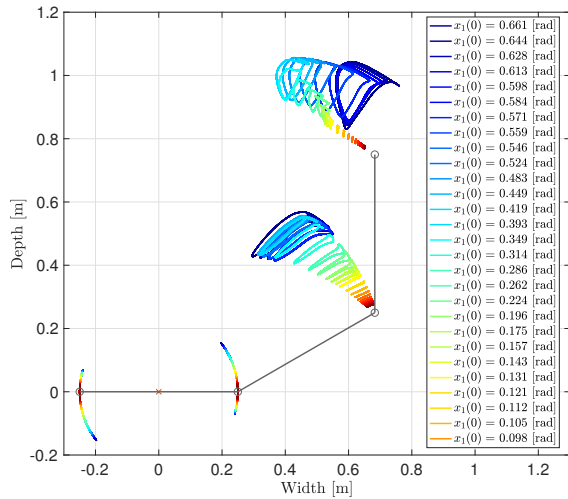

Fig. 9. Steady state oscillations obtained when applying the proposed controller (13) to stabilize different energy levels within a same Eigenmanifold of a 3 link planar manipulator. The first link rotates w.r.t. its center. These oscillations are produced without any injection of energy at steady state.

[11] A. Shiriaev, J. W. Perram, and C. Canudas-de Wit, "Constructive tool for orbital stabilization of underactuated nonlinear systems: Virtual constraints approach," *IEEE Transactions on Automatic Control*, vol. 50, no. 8, pp. 1164–1176, 2005.

[12] M. Maggiore and L. Consolini, "Virtual holonomic constraints for euler–lagrange systems," *IEEE Transactions on Automatic Control*, vol. 58, no. 4, pp. 1001–1008, 2012.

[13] G. Garofalo and C. Ott, "Passive energy-based control via energy tanks and release valve for limit cycle and compliance control," *IFAC-PapersOnLine*, vol. 51, no. 22, pp. 73–78, 2018.

[14] R. Ortega *et al.*, "Orbital stabilization of nonlinear systems via the immersion and invariance technique," *International Journal of Robust and Nonlinear Control*, vol. 30, no. 5, pp. 1850–1871, 2020.

[15] B. Yi *et al.*, "Orbital stabilization of nonlinear systems via mexican sombrero energy shaping and pumping-and-damping injection," *Automatica*, vol. 112, p. 108661, 2020.

[16] C. F. Sætre, A. Shiriaev, L. Freidovich, S. V. Gusev, and L. Fridman, "Robust orbital stabilization: A floquet theory-based approach," *arXiv preprint arXiv:2011.13674*, 2020.

[17] A. Banaszuk and J. Hauser, "Feedback linearization of transverse

[18] A. Kovaleva, *Optimal control of mechanical oscillations*. Springer Science & Business Media, 2013.

[19] J. Pen, W. Caarls, M. Wisse, and R. Babuška, "Evolutionary co-optimization of control and system parameters for a resonating robot arm," in *2013 IEEE International Conference on Robotics and Automation*. IEEE, 2013, pp. 4195–4202.

[20] J. Hwangbo, J. Lee, A. Dosovitskiy, D. Bellicoso, V. Tsounis, V. Koltun, and M. Hutter, "Learning agile and dynamic motor skills for legged robots," *Science Robotics*, vol. 4, no. 26, 2019.

[21] X. Liu, R. Gasoto, Z. Jiang, C. Onal, and J. Fu, "Learning to locomote with artificial neural-network and cpg-based control in a soft snake robot," in *2020 IEEE/RSJ International Conference on Intelligent Robots and Systems (IROS)*. IEEE, 2020, pp. 7758–7765.

[22] A. F. Vakakis, L. I. Manevitch, Y. V. Mikhlin, V. N. Pilipchuk, and A. A. Zevin, *Normal modes and localization in nonlinear systems*. Springer, 2001.

[23] D. Lakatos, W. Friedl, and A. Albu-Schäffer, "Eigenmodes of non-linear dynamics: Definition, existence, and embodiment into legged robots with elastic elements," *IEEE Robotics and Automation Letters*, vol. 2, no. 2, pp. 1062–1069, 2017.

[24] C. Della Santina and A. Albu-Schäffer, "Exciting efficient oscillations in nonlinear mechanical systems through eigenmanifold stabilization," *IEEE Control Systems Letters*, 2020.

[25] C. Della Santina, D. Calzolari, A. M. Giordano, and A. Albu-Schaffer, "Actuating eigenmanifolds of conservative mechanical systems via bounded or impulsive control actions," *IEEE Robotics and Automation Letters*, 2021.

[26] C. Della Santina, D. Lakatos, A. Bicchi, and A. Albu-Schäffer, "Using nonlinear normal modes for execution of efficient cyclic motions in articulated soft robots," *Proc. Int. Symp. on Experimental Robotics - ISER*, 2020.

[27] D. Calzolari, C. Della Santina, and A. Albu-Schäffer, "Pd-like regulation of mechanical systems with prescribed bounds of exponential stability: the point-to-point case," *IEEE Control Systems Letters*, 2020.

[28] A. Albu-Schaffer, D. Lakatos, and S. Stramigioli, "Strict nonlinear normal modes of systems characterized by scalar functions on riemannian manifolds," *IEEE Robotics and Automation Letters*, 2021.

[29] S. W. Shaw and C. Pierre, "Normal modes for non-linear vibratory systems," *Journal of sound and vibration*, vol. 164, no. 1, pp. 85–124, 1993.

[30] A. F. Filippov, *Differential equations with discontinuous righthand sides: control systems*. Springer Science & Business Media, 2013, vol. 18.

[31] R. Goebel, R. G. Sanfelice, and A. R. Teel, "Hybrid dynamical systems," *IEEE Control Systems*, vol. 29, no. 2, pp. 28–93, 2009.

[32] L. H. Duc, A. Ilchmann, S. Siegmund, and P. Taraba, "On stability of linear time-varying second-order differential equations," *Quarterly of applied mathematics*, vol. 64, no. 1, pp. 137–152, 2006.

dynamics for periodic orbits," *Systems & control letters*, vol. 26, no. 2, pp. 95–105, 1995.